VOL.40 Nº1 2023
https://doi.org/10.22491/rmct.v40i1.8902.en

Analysis of glass substituted hydroxyapatite under different sintering routes

Andrey Mariano dos Santos[1], Iana Costa Carvalho[1], Ygor Pereira de Lima[1], Amal Elzubair[1]*, Suzana Noronha Ferreira Ribeiro[1], André Luís de Vasconcelos Cardoso[1], Marcelo Henrique Prado da Silva[1]
[1]Instituto Militar de Engenharia.
Praça General Tibúrcio, 80 - Urca, Rio de Janeiro - RJ, 22290-270
***amal@ime.eb.br**

ABSTRACT: Hydroxyapatite is a calcium phosphate that is classified as a biomaterial. It is used in bone restorations as it has characteristics similar to the mineral phase of bone tissue. Substitutional apatites have been especially researched to obtain better parameters for their syntheses and improve their impact on final applications. In view of the importance of these compounds as a biomaterial, this research aimed to study sintered substituted hydroxyapatite compounds to identify the formed phases, their microstructure, morphology, and shrinkage after sintering. HA and a composite of HA with 4% calcium phosphate and magnesium-based glass were produced from precursors in solutions and then sintered at different temperature. Results were obtained regarding the phases present and their morphology for the different conditions of chemical composition and sintering route by XRD analysis and scanning electron microscopy. Density and diameter shrinkage were analyzed after green body sintering at 1350 ºC. The HA samples showed a hexagonal phase, greater density, greater shrinkag, and uniform morphology with fewer pores than the HA/glass composite samples. The addition of magnesium glass partially transformed HA into tricalcium phosphate.

KEYWORDS: Biomaterial, Hydroxyapatite, Glass, XRD, Microstructure.

RESUMO: A hidroxiapatita é um fosfato de cálcio classificado como biomaterial utilizado em restaurações ósseas, dado que apresenta características similares à fase mineral do tecido ósseo. Em particular, as apatitas substitucionais vêm sendo pesquisadas a fim de se obter melhores parâmetros de suas sínteses e, consequentemente, de seu impacto na aplicação final. Tendo em vista a importância desses compostos como biomateriais, a presente pesquisa teve o objetivo de estudar compostos sinterizados de hidroxiapatita substituída, visando identificar as fases formadas, a morfologia da microestrutura e a retração do material após sinterização. HA e um compósito de HA e 4% de vidro a base de fosfato com cálcio e magnésio, produzidos a partir de precursores em soluções e depois sinterizadas em diferentes patamares de temperatura. Resultados foram obtidos quanto às fases presentes e sua morfologia para as diferentes condições de composição química e rota de sinterização aplicada a partir da análise de DRX, microscopia eletrônica de varredura. A densidade e a retração de diâmetro foram analisadas após a sinterização dos corpos verdes à 1350 ºC. As amostras da HA apresentaram uma fase, maior densidade, maior retração e morfologia uniforme com poucos poros, comparada às amostras do compósito HA/vidro. A adição de vidro de magnésio resultou na transformação parcial da HA em fosfato tricálcico.

PALAVRAS-CHAVE: Biomaterial, Hidroxiapatita, Vidro, DRX, Microestrutura

1. Introduction

Increasingly interest has been devoted to calcium phosphate materials because of a chemical composition similar to that of the bone mineral. Thus, calcium phosphate ceramics with expected superior biological properties began to be investigated. They are called bioactive ceramics, a family that mainly includes calcium phosphate, so-called hydroxyapatite (HA), tricalcium phosphate (TCP), and biphasic calcium phosphates (BCP, the mixture of HA and TCP). Hydroxyapatite is considered the most used biomaterial in bone restorations [1-3]. Given that there are several methods of obtaining this compound in the literature, the synthesis of hydroxyapatite powder is of commercial and scientific interest, as the processing conditions have a direct influence on the structure, morphology and application of the desired final compound [4].

In addition, hydroxyapatite may act as a coating for orthopedic implants in physiological media. It is also noted that its application in dental implants is feasible, as well as calcium and phosphorus reserves, considering the ease of anion and cation substitutions, providing the release or storage of ions in body fluids [5].The porosity of hydroxyapatite is responsible for the adsorption capacity of molecules, favoring the incorporation of drug-conducting drugs [3], as HA

easily substitutes anions and cations. Thus, bone growth around the implant is also promoted [6].

This work aimed to process HA in different routes, using samples of pure hydroxyapatite, as well as hydroxyapatite with a glass based on calcium and magnesium phosphate, in order to identify phases formed and morphology of the microstructure.

2. Materials and Methods

2.1 Glass Synthesis

For the production of glass, individual solutions of the precursors $MgCl_2.6H_2O$ 99.99%, $CaCO_3$ 99.99%, $H_3PO_4$85% were prepared to meet the proportion of 0.01 mol Mg: 0.03 mol, Ca: 0.06 mol, P.

The amount of 3.033 g of $CaCO_3$, 2.033 g of $MgCl_2.6H_2O$ were weighed on a Gehaka analytical balance, model BK 300, and 8.08 ml of H_3PO_4 were measured in a beaker, all reagents measured. Then they were diluted in distilled water separately, totaling 50 ml of solution for each. The solutions were then mixed in a 500 ml Becker with magnetic stirrer with heater marca 5L-HS9T.

2.2 Sintering of samples

Four samples were prepared, two with pure hydroxyapatite (HA) and two composite samples with 96% hydroxyapatite and 4% magnesium glass (HA/glass composite). For this, 11.95 g of hydroxyapatite was weighed for the pure tablets, 11.87 g of hydroxyapatite and 0.49 g of magnesium phosphate glass for the composite tablets. The hydroxyapatite used was previously synthesized in the ceramic laboratory. The composite powders were ground in a MARCONI horizontal ball mill, model MA 500.

Tablets of 2 g were produced in a 20 cm diameter matrix, initially pressed in a manual hydraulic press with a load of 2 tons applied for 30 s, totaling a load of 62.38 MPa. Subsequently, the pellets were sintered in the Jung oven, and the samples were sintered in pairs consisting of an HA pellet and one of the HA/glass composite, at two different temperatures: 1100°C and 1350°C.

Figure 1 shows the sintering route in which the furnace was first heated to 1000°C with a heating rate of 10°C/min. When stabilized at this temperature, heating was continued until the sintering temperature with a heating rate of 3°C/min, and then remained at this temperature for 3 hours.

Figure 1 - Schematic representation of the sintering route.

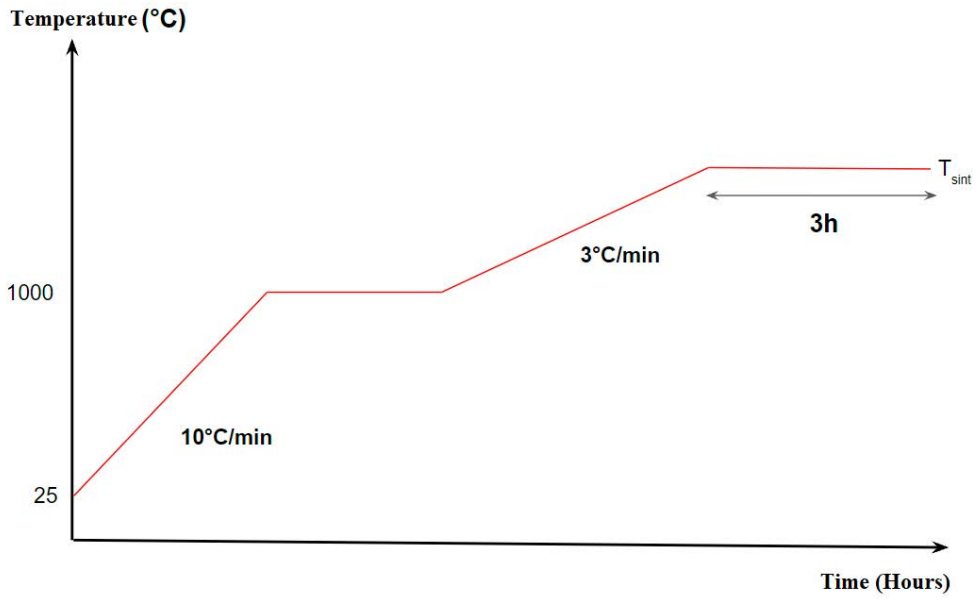

3. Characterization of samples

3.1 Physical Properties

The linear contraction, bulk density and porosity of the samples were measured. The measurement of linear contraction was performed with the aid of a manual caliper, of the diameters of the samples in the green body condition and after sintering. The density and porosity were calculated by the Archimedes method applied to the sintered samples:

$$\text{Bulk density} = (M_{dry}).\rho_{water} / (M_{wet} - M_{immersed}) \quad (1)$$

$$\text{Porosity \%} = (M_{wet} - M_{dry}) \times 100 / (M_{wet} - M_{immersed}) \quad (2)$$

Where: M is the mass of the sintered sample, measured dry, immersed and wet.

ρ_{water} is the density of water ~ 1 g/cm^3.

3.2 Scanning Electron Microscopy (SEM)

The morphologies and microstructure analyses were performed with the Scanning Electron Microscope, QUANTA model FEG 250 (SEM-FEG). The following parameters were used: 10 to 15 kV acceleration voltage, 30 µs scan time, 1000 to 16,000 X magnification. In addition, the technique was applied with secondary electrons.

3.3 X-Ray Diffraction

Crystallographic phase analyses were performed using X-ray diffraction (XRD) with a Panalytical diffractometer, model X'Pert PRO MRD. Cobalt source (Co-Kα = 1.789010 Å), 40 kV voltage, 40 mA current, 2θ scan from 20° to 80° under 0.029° step was used.

4. Results and discussion

4.1 Physical Properties

Table 1 shows the contraction content of the samples after sintering. It was not possible to obtain the contraction value of the sintered samples at 1100 °C, as they fractured after the process. When HA and HA/glass densification above 1000 °C is initiated, grain contours form [7], total pore volume decreases, and samples contract to reach their maximum bulk density. Then, the linear contraction occurs due to the compaction of the grains that make up the ceramic material during the sintering process, increasing the density of the material and consequently decreasing its dimensions.

It is seen that the percentage of contraction for the pure HA samples was much higher than that of HA/glass, indicating that the presence of the glass promoted a drop to more than half contraction of the sintered sample.

Density measurements (Table-1) revealed that samples of the pure HA sintered at 1350ºC have higher density than that of the HA/sintered glass composite at the same temperature. This resulted in a higher porosity in the composite when compared to that of pure HA.

Samples sintered at 1100ºC had lower density and higher porosity than those sintered at 1350ºC.

Table 1 - Linear contraction, density and porosity of sintered samples.

Sample	Contraction ± SD (%)	Density ± SD (g/cm^3)	Porosity ± SD (%)
HA (1350ºC)	19.10 ± 0.34	2.7769 ± 0.0291	2.96 ± 0.48
HA/Glass (1350ºC)	8.8 ± 0.94	2.5472 ± 0.0034	9.47 ± 1.42
HA (1100ºC)	-	2.434	15.56
HA/Glass (1100ºC)	-	1.7982	37.69

4.2 Scanning Electron Microscopy (SEM)

Figures 2 to 5 show the micrographs of the sintered samples obtained by SEM. Figures 2 and 3 show HA and HA/glass samples sintered at 1100 °C. In Figures 2a and 3a, it is possible to see crack formation in the samples, but with greater intensity in the HA/glass composite. It is observed in Figures 2b and 3b that there was a growth and coalition of the grains in the process, thus decreasing the total interfacial energy of the grain contours. It can be noted that the HA/glass composite grains have greater growth and have a significant presence of pores.

Figure 2 - Microstructure of the pure HA sample sintered at 1100°C.

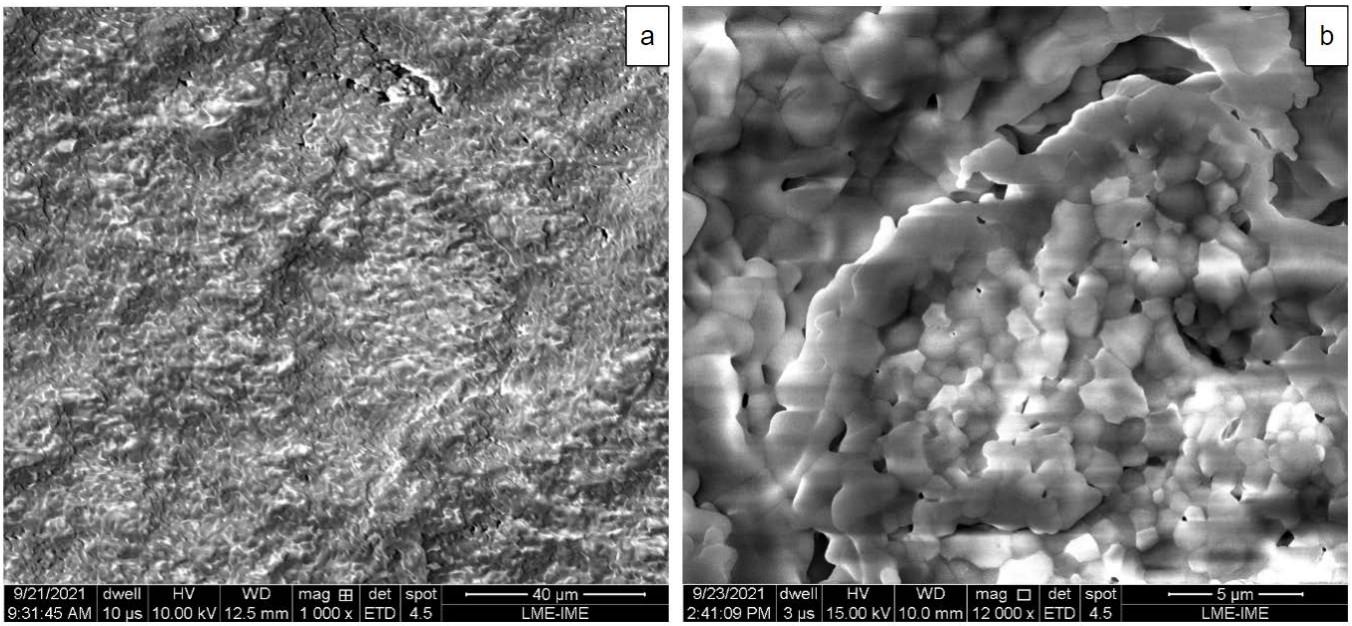

Figure 3 - Microstructure of the HA/Sintered glass sample at 1100°C.

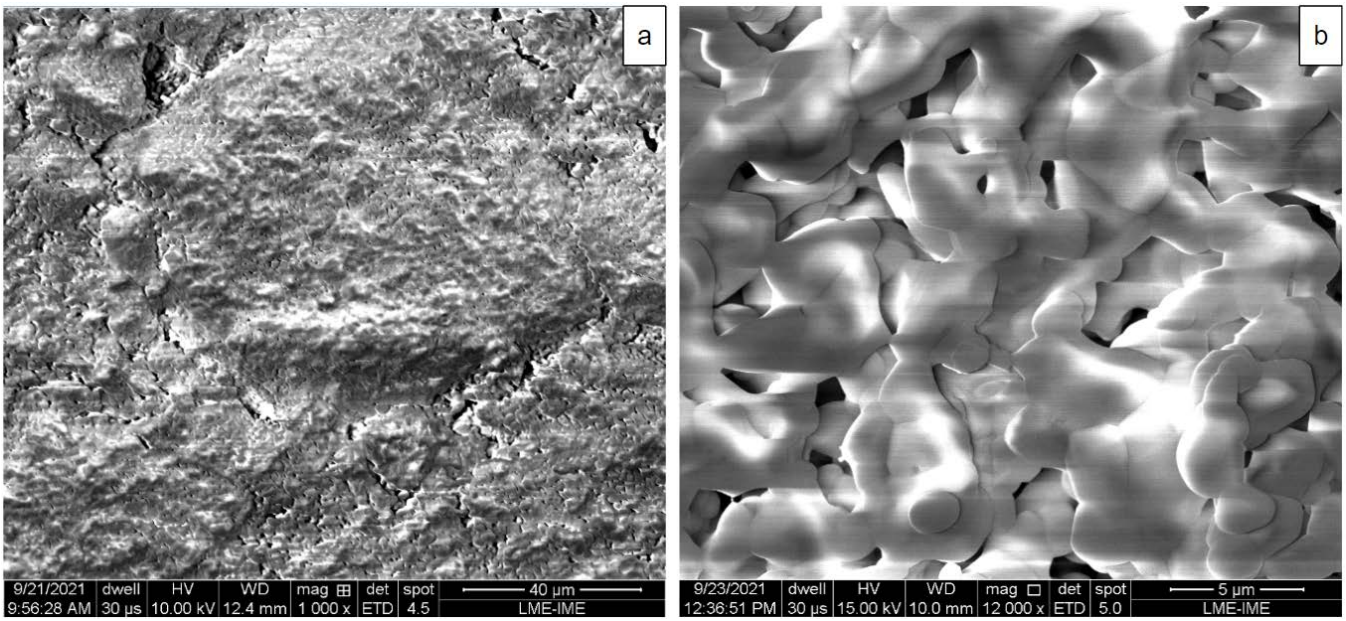

In the case of the samples sintered at 1350°C, a less rough surface appearance morphology was observed in Figures 4a and 5a than in the samples sintered at 1100°C. There is also a lower occurrence of cracks and greater densification. There are still some intergranular pores and channels, most notably in the HA/glass samples (Figure 5a). Figure 4a shows that HA sintering produced ceramic, almost ideally dense (bulk density ~ 97% as shown in Table-1), without significant grain growth. The final microstructure in Figures 4a and 5a consists of hexagonal grains. Figure 4b showed regions with residual closed pores. An interesting structure can be seen in Figure 5b, with increase magnification, there is presence of pores or small circular cavities distributed on the surface of the grains.

Figure 4 - Microstructure of the pure HA sample sintered at 1350°C.

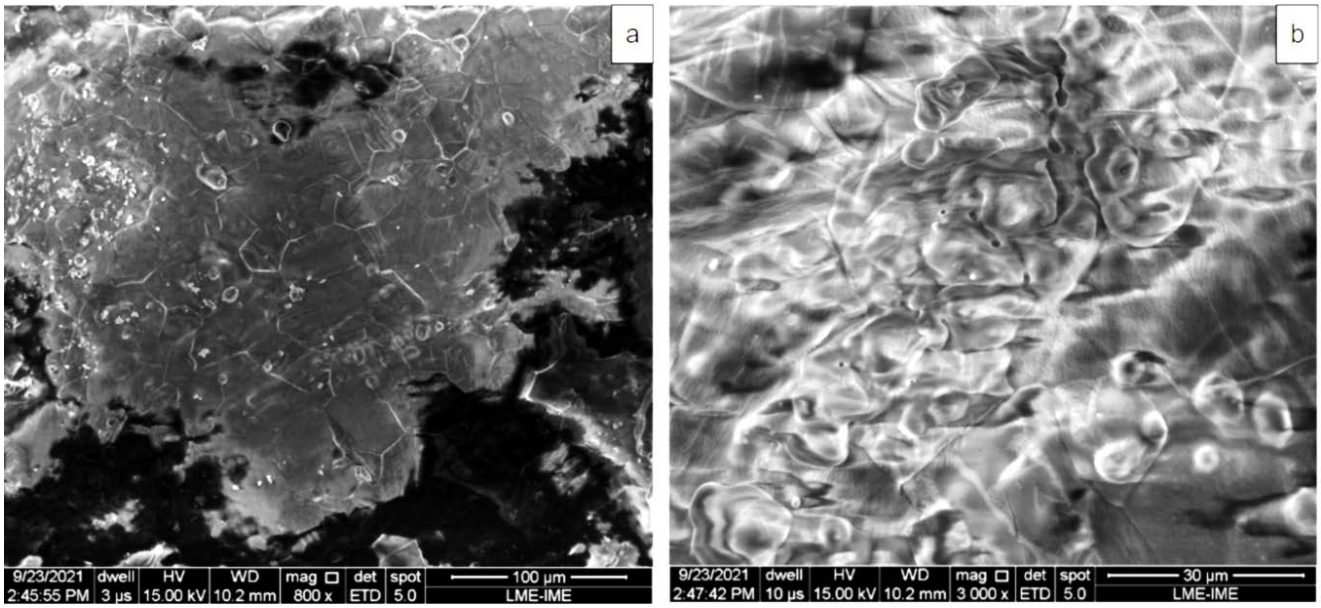

Figure 5 - Microstructure of the HA/glass sample sintered at 1350 °C.

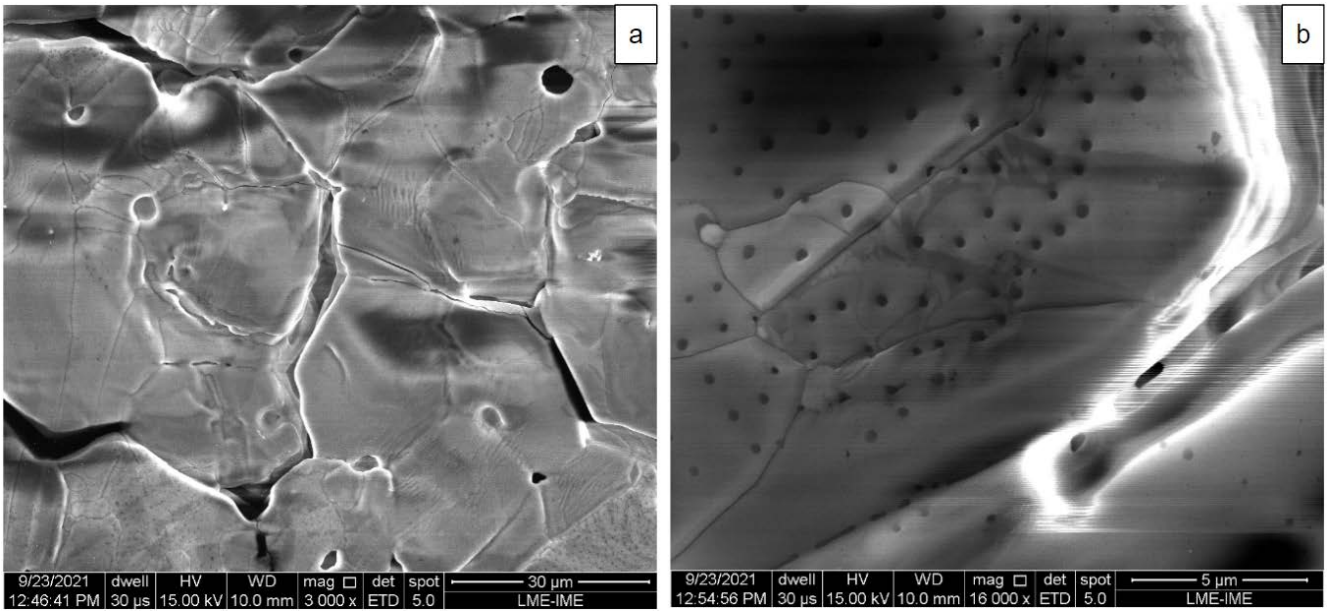

4.3 X-Ray Diffraction

The X-Ray Diffraction measurements resulted in the diffractograms of Figure 6. In the case of the pure HA sample sintered at 1100 °C, a majority hydroxyapatite phase and another unidentified minority phase were identified. In the pure HA sample sintered at 1350°C, the formation of a single crystalline phase of hydroxyapatite was observed (JCPDS 09-0432).

In both cases, the indexed HA phase has hexagonal symmetry and lattice parameters of a = b = 9.4180 Å and c = 6.8840 Å. This result is compatible with the hexagonal microstructure of Figure 4a.

Figure 6 - XRD diffractograms of sintered samples at 1100ºC and 1350ºC.

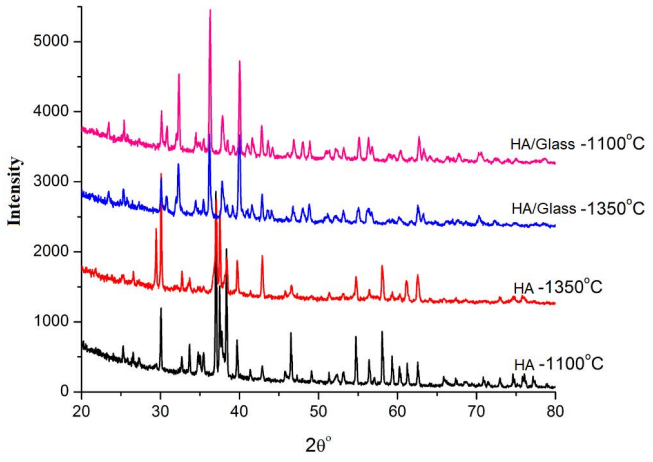

The HA/glass samples, on the other hand, presented the same crystalline structure at the two sintering temperatures, a pattern different from pure HA, being better indexed by the rhombohedral phase (JCPDS 09-0169) of the β-TCP, with lattice parameters of a = b = 10.4290 Å and c = 37.3800 Å. This indicates that HA has partially transformed into β-TCP (β-tricalcium phosphate $Ca_3(PO_4)_2$). Thus, the substitution of Ca^{2+} in the crystal lattice of the HA by Mg^{2+} favors the thermal decomposition of the HA into a biphasic mixture of HA and TCP [8, 9]. Magnesium also stabilized this transformation at both sintering temperatures.

It is noted that the lattice parameter c of the samples with glass addition is much higher than for the pure HA phase. This difference is consistent with the result of linear contraction, which may be the cause of the observed effect of greater retraction of pure HA samples in relation to that of the composite.

Conclusions

From these analyses, the following conclusions can be cited:

- The production of HA and glass based on calcium and magnesium phosphate under the use of precursors in liquid medium ensured the homogeneity of the compounds;
- The contraction of the surface area after sintering indicates the coalescence of the grains of the green body, elimination of pores and consequently densification. The pure HA samples had higher bulk density and lower porosity than the HA/glass composite at the same temperature, meaning that the addition of glass slows the densification of the HA;
- There was a growth, coalition of the grains and formation of grain contours in the sintering process at both temperatures. The HA/glass composite had higher grain growth, presence of pores and intergranular channels assimilate cracks;
- The microstructure of the HA samples at 1350ºC showed the grains in hexagonal shape, which was confirmed by XRD, with hexagonal crystal structure. While the HA/glass composite had rhombohedral crystal structure which indicates that HA partially transformed into β-TCP due to partial replacement of calcium with magnesium.

Acknowledgments

This work was carried out entirely on the premises of the IME. The authors would like to thank the funding agencies, CAPES and CNPq, for their financial support.

Authorship and Collaborations

All authors participated equivalently in the article preparation.

References

[1] Hench, L. L.; Polak, J. M. Third-generation biomedical materials. *Science*, [*s. l.*], v. 295, p. 1014– 1017, 2002.
[2] Jarcho, M. Calcium phosphate ceramics as hard tissue prosthetics. *Clinical Orthopaedics and Related Research*, [*s. l.*], v. 157, p. 259–78, 1981.
[3] Groot, K de. *Bioceramics of calcium phosphate*. Boca Raton: CRC Press, 1983.
[4] Viana, J. R. *et al*. Análise comparativa da síntese de hidroxiapatita via estado sólido. *Matéria*, Rio de Janeiro, v. 25, n. 1, 2020. DOI: https://doi.org/10.1590/S1517-707620200001.0914
[5] Sygnatowicz, M.; Keyshar, K.; Tiwari, A. Antimicrobial Properties of Silver-doped Hydroxyapatite nano-powders and Thin Films. *Biological Biomedical Materials*, [*s. l.*], v. 62, p. 65-70, 2010.
[6] Santos, M. V. B.; Osajima, J. A.; Silva-Filho, E. C. Hidroxiapatita: suporte para liberação de fármacos e propriedades antimicrobianas. *Cerâmica*, [*s. l.*], v. 62, p 256-265, 2016.
[7] Rootare, H. M.; Craig, R. G. Characterization of hydroxyapatite powders and compacts at room temperature and after sintering at 1200ºC. *Journal of Oral Rehabilitation*, [*s. l.*], v. 5, n. 3, p. 293–307, 1978.
[8] Cacciotti, I.; Bianco, A.; Lombardi, M.; Montanaro, L. Mg-substituted hydroxyapatite nanopowders: Synthesis, thermal stability and sintering behaviour. *Journal of the European Ceramic Society*, [*s. l.*], v. 29, n.14, p. 2969–2978, 2009.
[9] Gibson, I.R.; Bonfield, W. Preparation and characterization of magnesium/carbonate co-substituted hydroxyapatites. *Journal of Materials Science: Materials in Medicine*, [*s. l.*], v. 13, n. 7, p. 685–93, 2002.